Supplement of Atmos. Chem. Phys., 24, 9355–9368, 2024
https://doi.org/10.5194/acp-24-9355-2024-supplement

Atmospheric Chemistry and Physics
Open Access

Supplement of

Atmospheric NH_3 in urban Beijing: long-term variations and implications for secondary inorganic aerosol control

Ziru Lan et al.

Correspondence to: Weili Lin (linwl@muc.edu.cn)

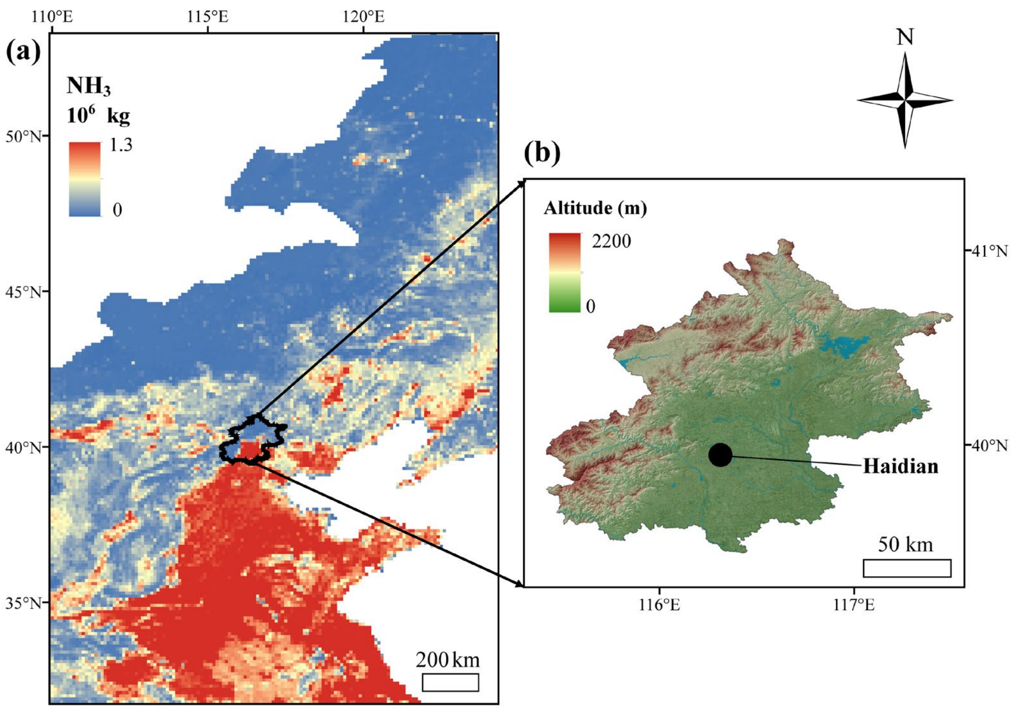

Figure S1. NH_3 emission in and around Beijing (a) and topographic map of Beijing (b). The NH_3 emissions data represent the total for 2017, sourced from emission inventories (Huang et al., 2012; Kang et al., 2016).

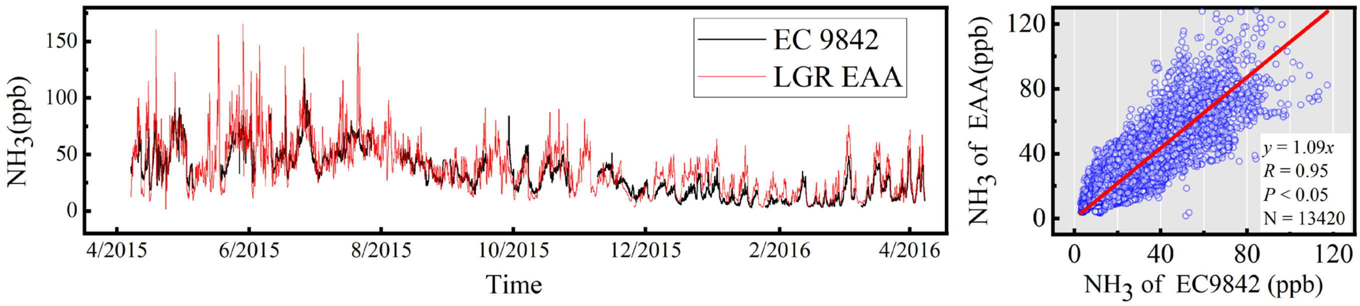

Figure S2. The result of parallel observation made by two analyzers.

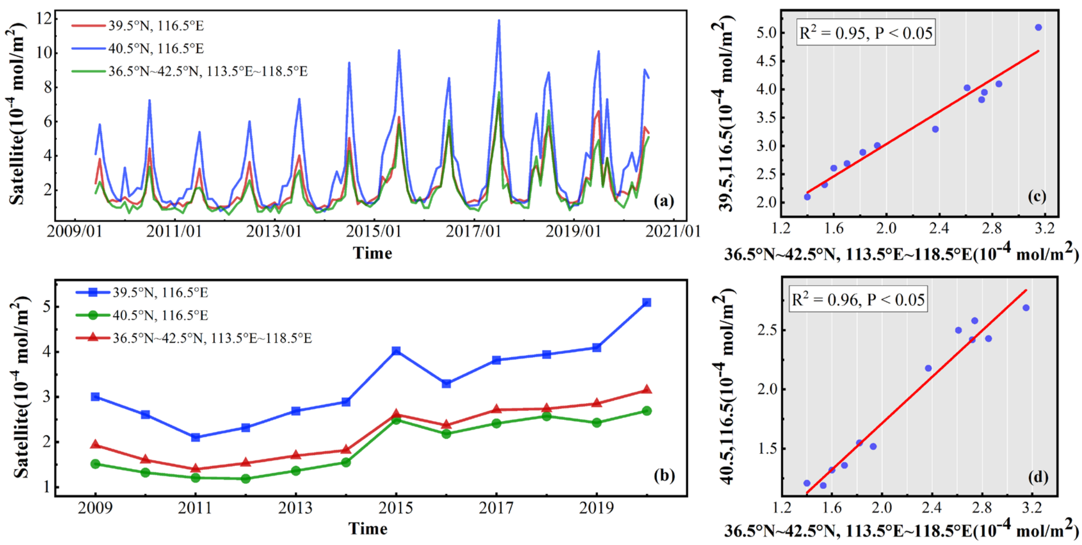

Figure S3. Monthly (a) and annual (b) variations and correlations between satellite observations during the observation period at the grid points around the monitoring stations (39.5°N, 116.5°E and 40.5°N, 116.5°E) (c) and the average observations in the region selected for the present study (36.5°N~42.5°N, 113.5°E~118.5°E) (d).

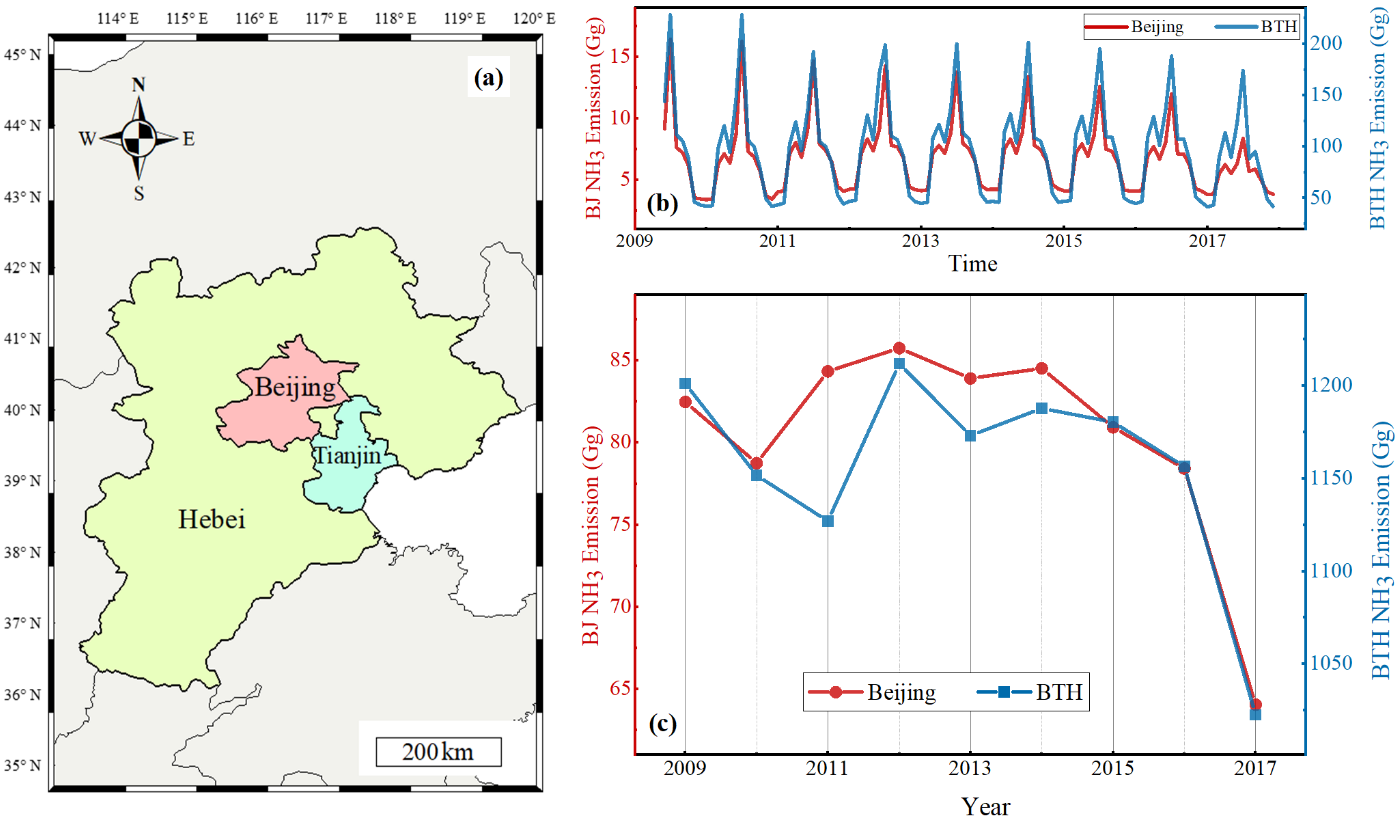

Figure S4. Comparison of NH_3 emissions in Beijing (BJ) with those in the Beijing-Tianjin-Hebei Region (BTH) during the observation period. (a) Geographic location of BTH, (b) Monthly emissions of atmospheric NH_3 in Beijing and BTH from 2009 to 2017, (c) Annual emissions of atmospheric NH_3 in Beijing and BTH from 2009 to 2017.

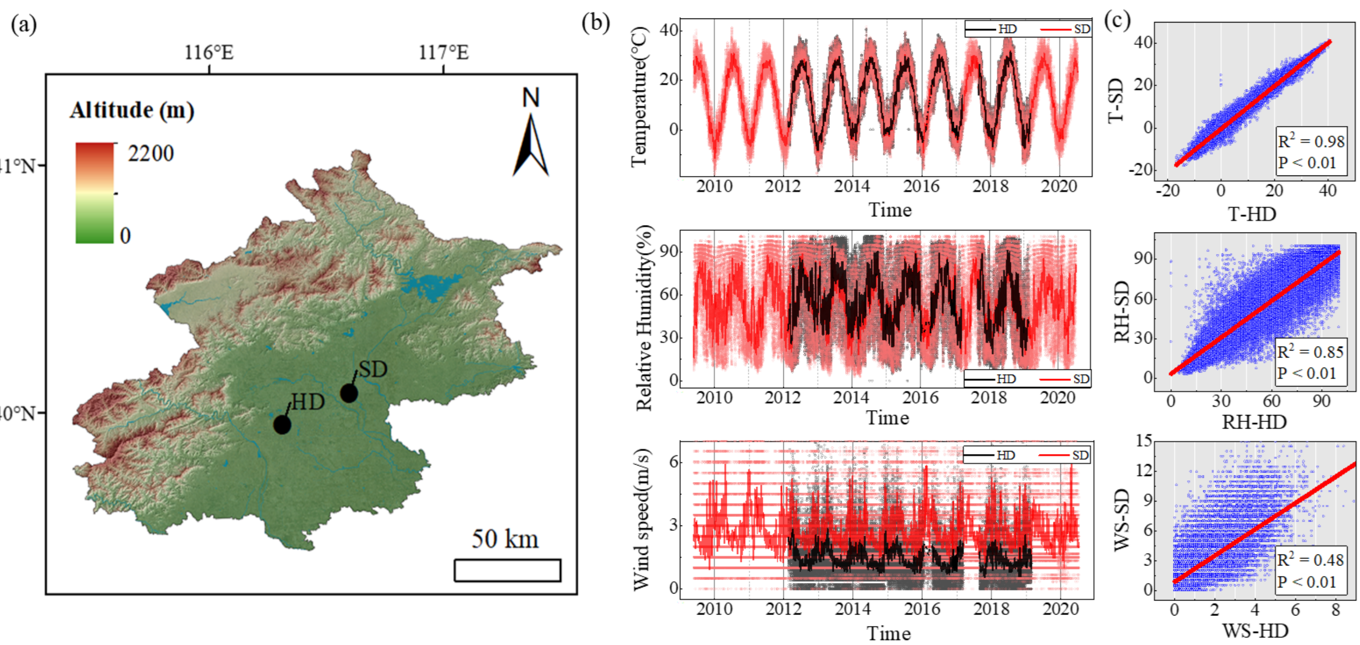

Figure S5. Comparison of meteorological elements between the meteorological station at the capital airport (SD) and the Haidian meteorological station (HD). (a) Geographic locations of SD and HD; (b) Time series plots of temperature, relative humidity, and wind speed for SD and HD, with hollow points as hourly averages and solid lines as two-week smoothed curves, (c) Correlation of temperature, relative humidity, and wind speed between SD and HD.

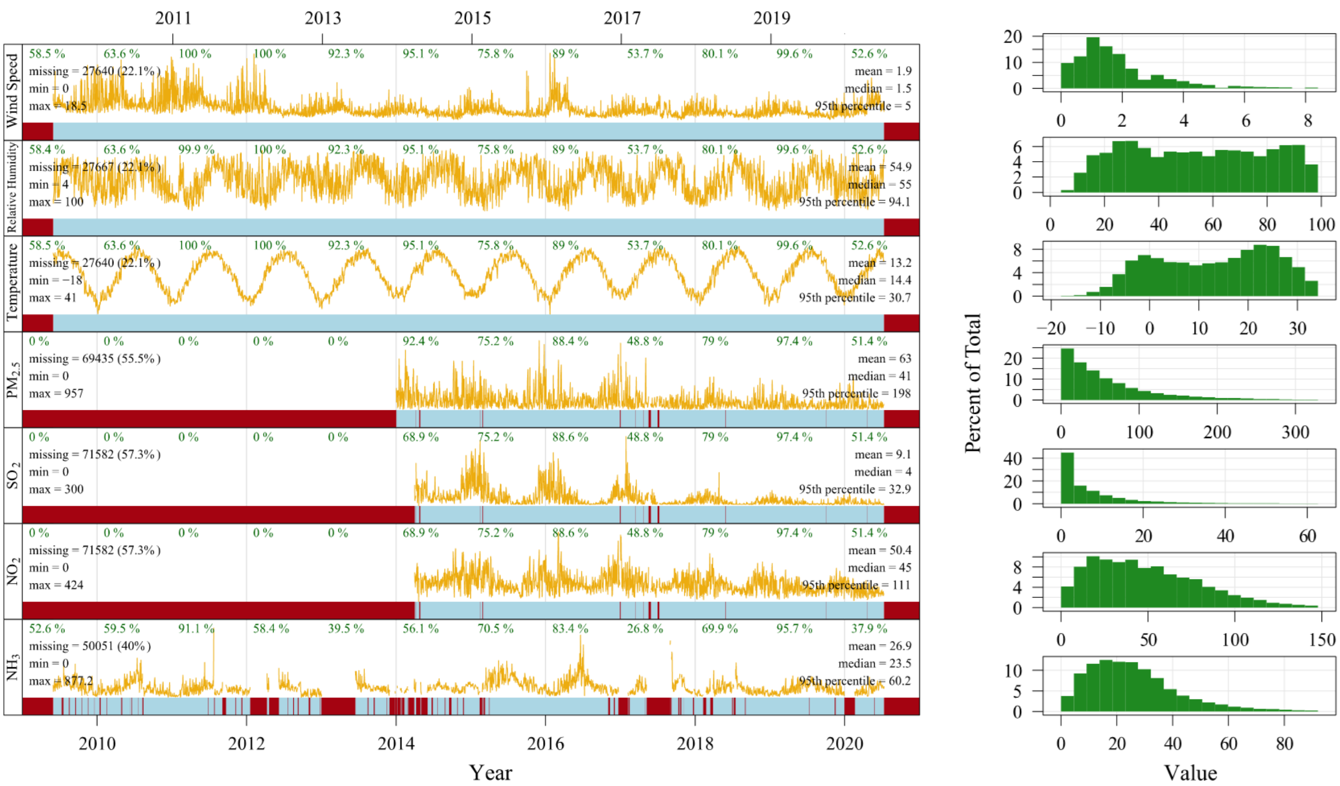

Figure S6. Time series, frequency distributions, and statistical analysis of NH_3 mixing ratios (ppb), selected pollutant concentrations (μg/m^3), and selected meteorological data (Wind speed: m/s, Relative humidity: %, Temperature: °C) during the observation period (mean, median/95% quartile, minimum/large values, and amount and percentage of missing value data).

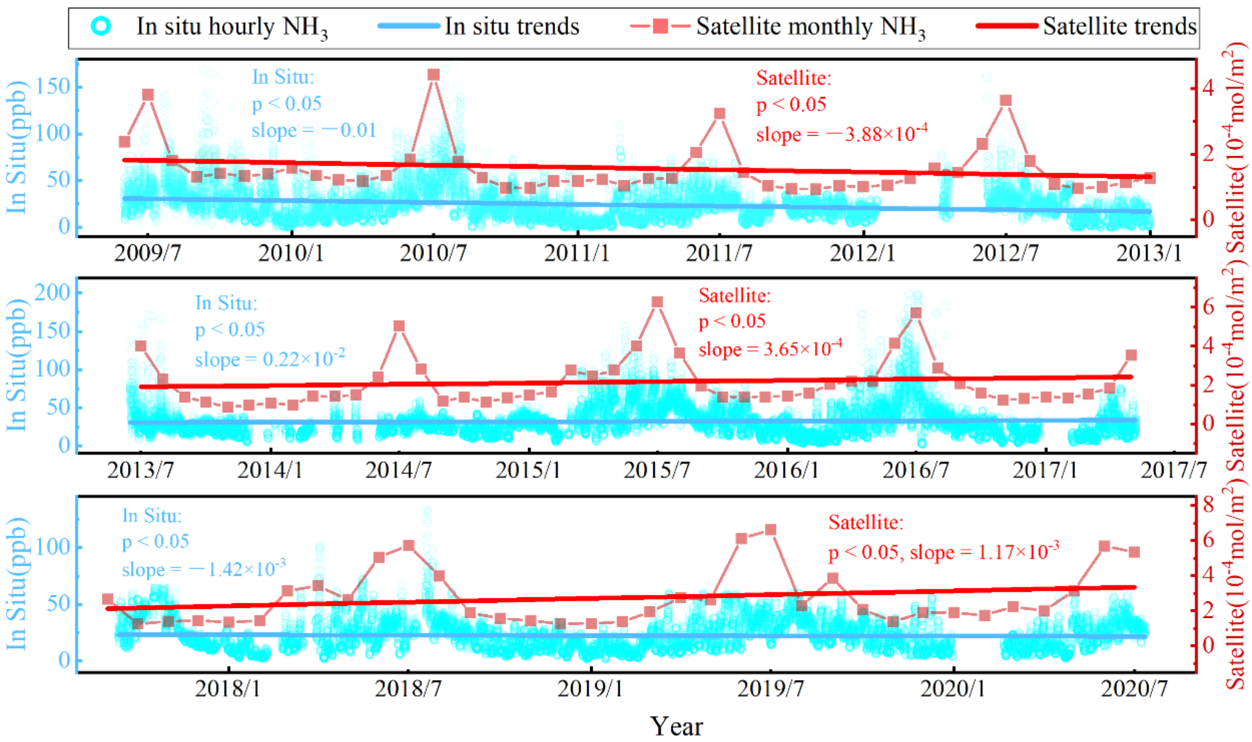

Figure S7. Trends in atmospheric NH_3 concentrations observed in situ and by satellite from June 2009 to January 2013, from June 2013 to May 2017, and from September 2017 to July 2020.

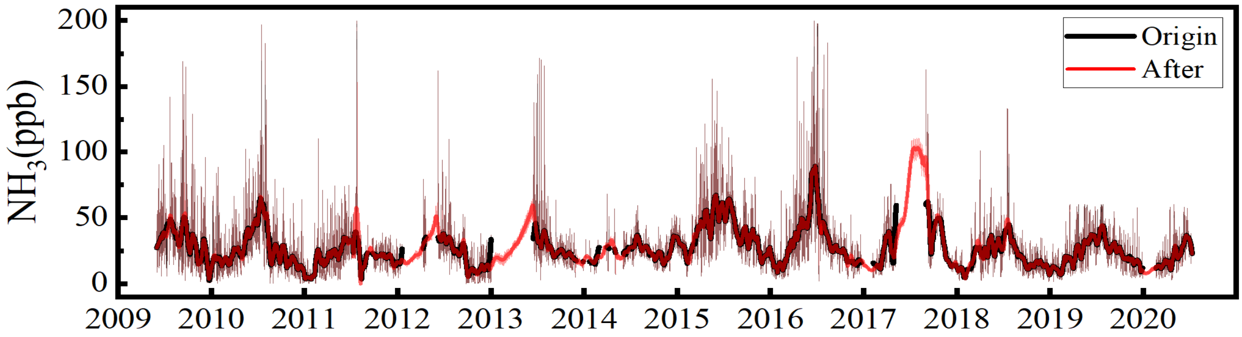

Figure S8. Raw data on NH_3 mixing ratios during the observation period and data with missing values filled in after Random Forest Model calculations.

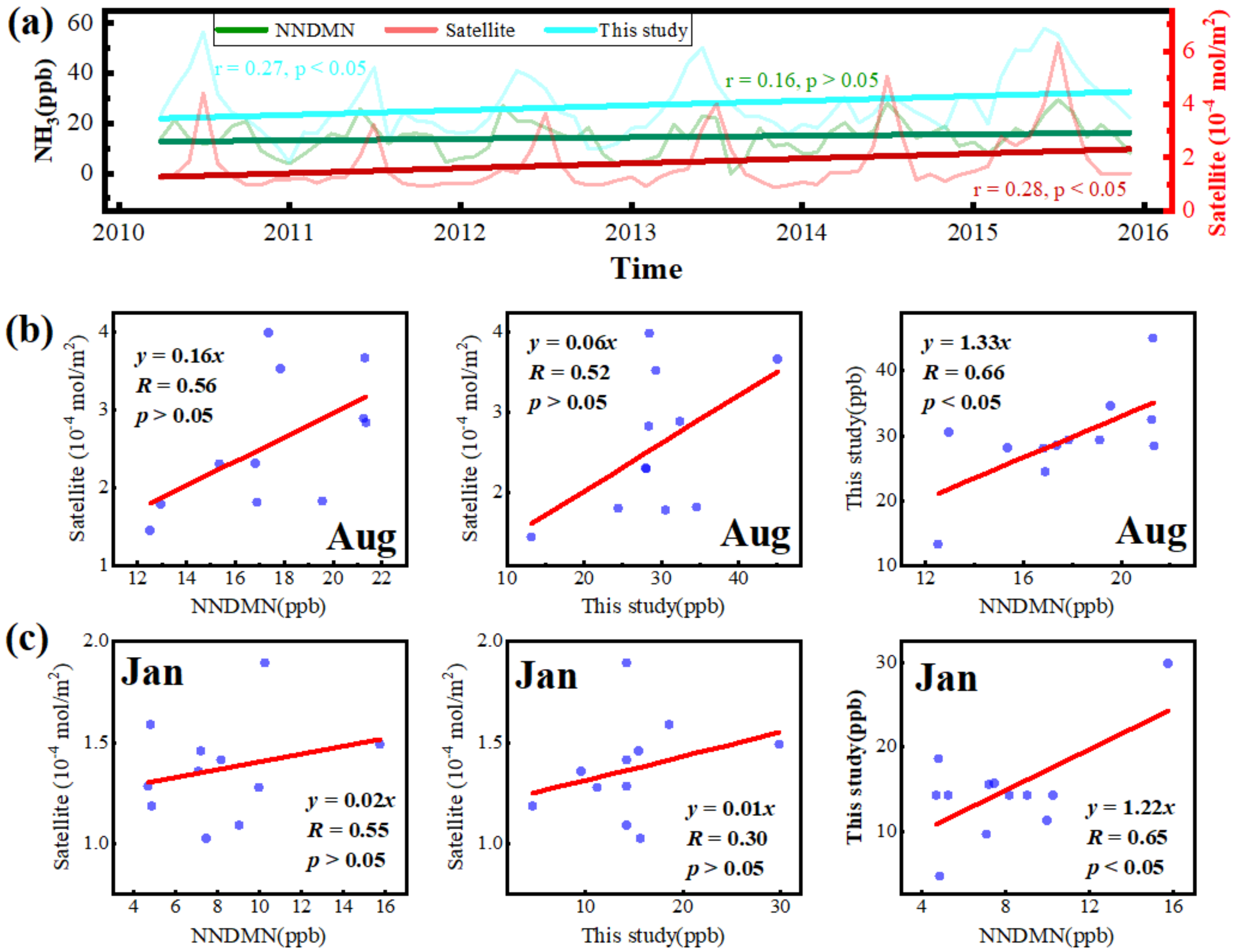

Figure S9. (a) Atmospheric NH_3 monthly average concentrations observed in this study, NNDMN Beijing station, and by satellite in Beijing urban area and their trends from April 2011 to December 2015. (b) Correlations between NH_3 concentrations observed in this study, NNDMN, and by satellite from January 2009 to January 2020. (c) Correlations between NH_3 concentrations observed in this study, NNDMN, and by satellite from January 2009 to August 2020.

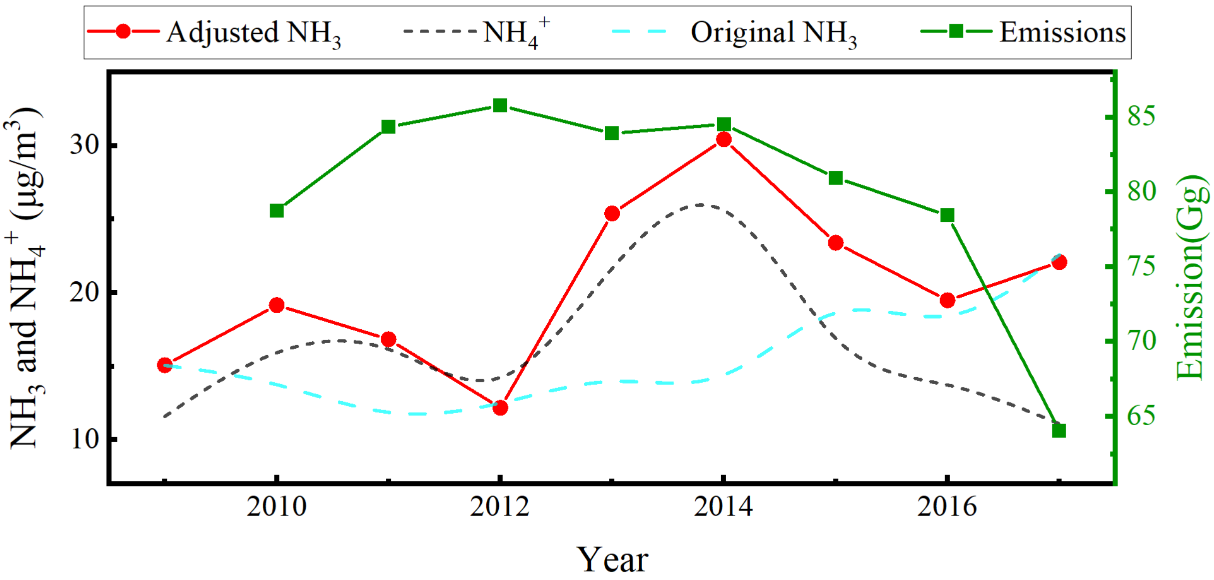

Figure S10. Annual averages of atmospheric NH_3, NH_4^+ in $PM_{2.5}$, and adjusted atmospheric NH_3 and NH_3 emissions in Beijing urban area from 2010 to 2017

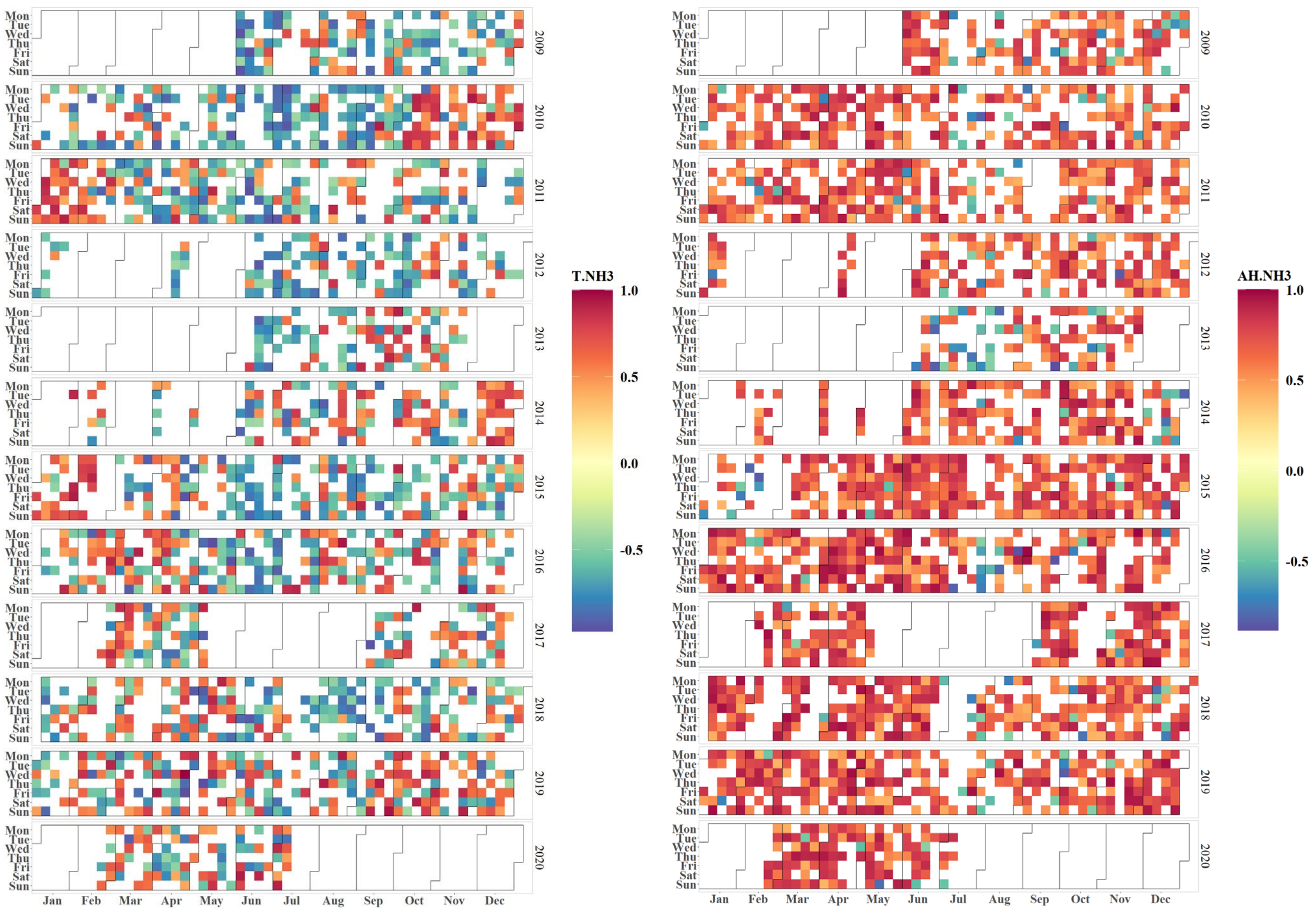

Figure S11. Correlation between daily temperature and NH_3 mixing ratio (left) and between absolute humidity and NH_3 concentration (right) for the observation period.

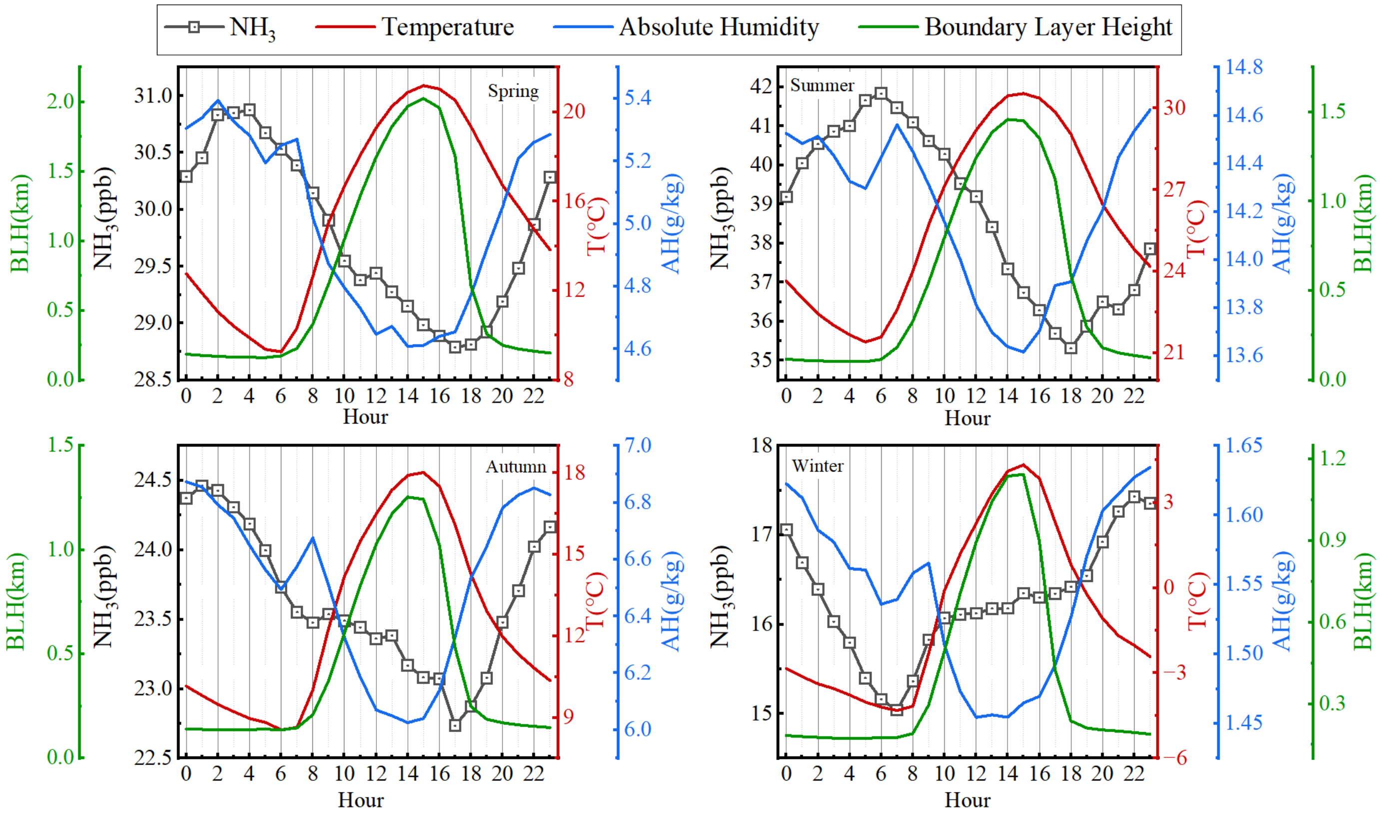

Figure S12. Average diurnal variations in NH_3, temperature, absolute humidity and boundary layer height in different seasons in Beijing urban area. Boundary layer height data are from the ERA5 global atmospheric reanalysis (Hersbach et al., 2023).

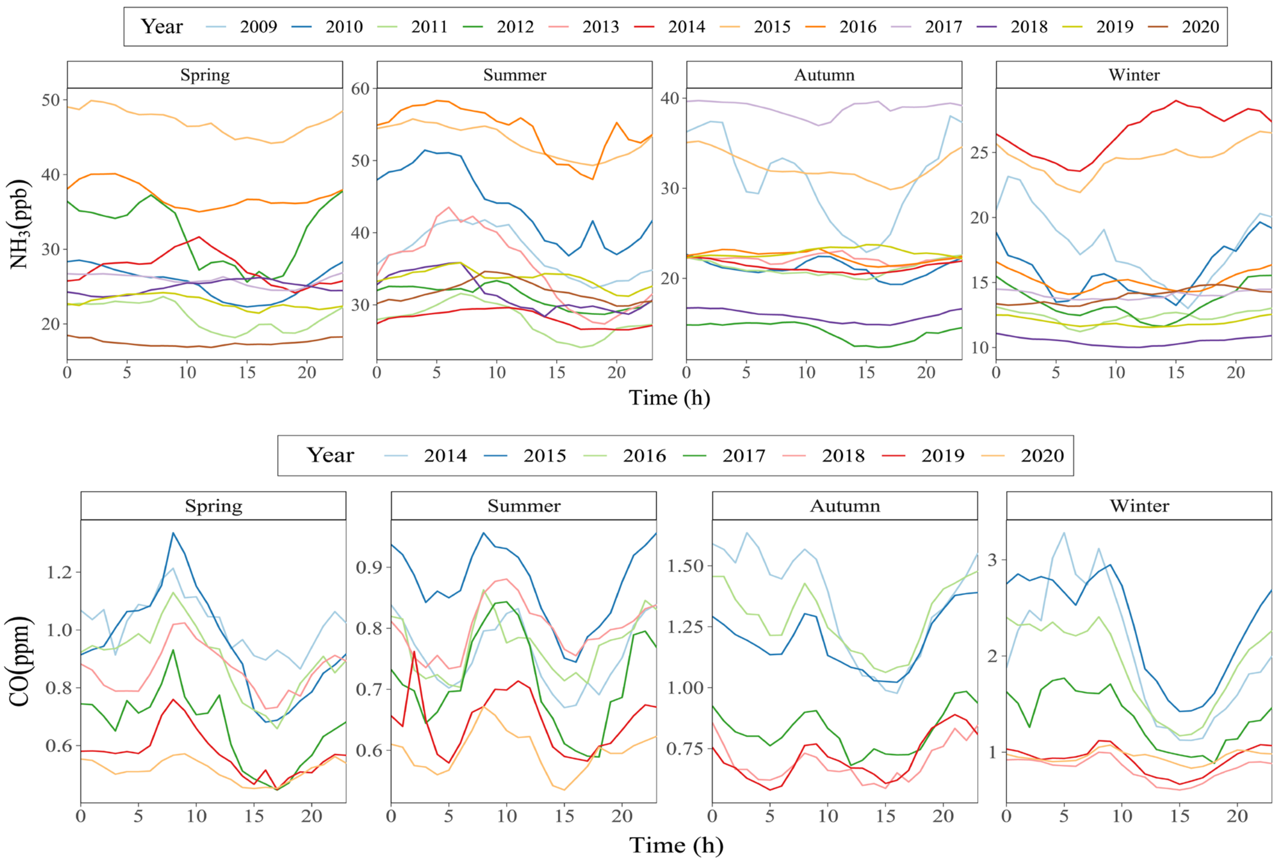

Figure S13. Characteristics of daily variations in NH_3 and CO in different years and seasons during the observation period.

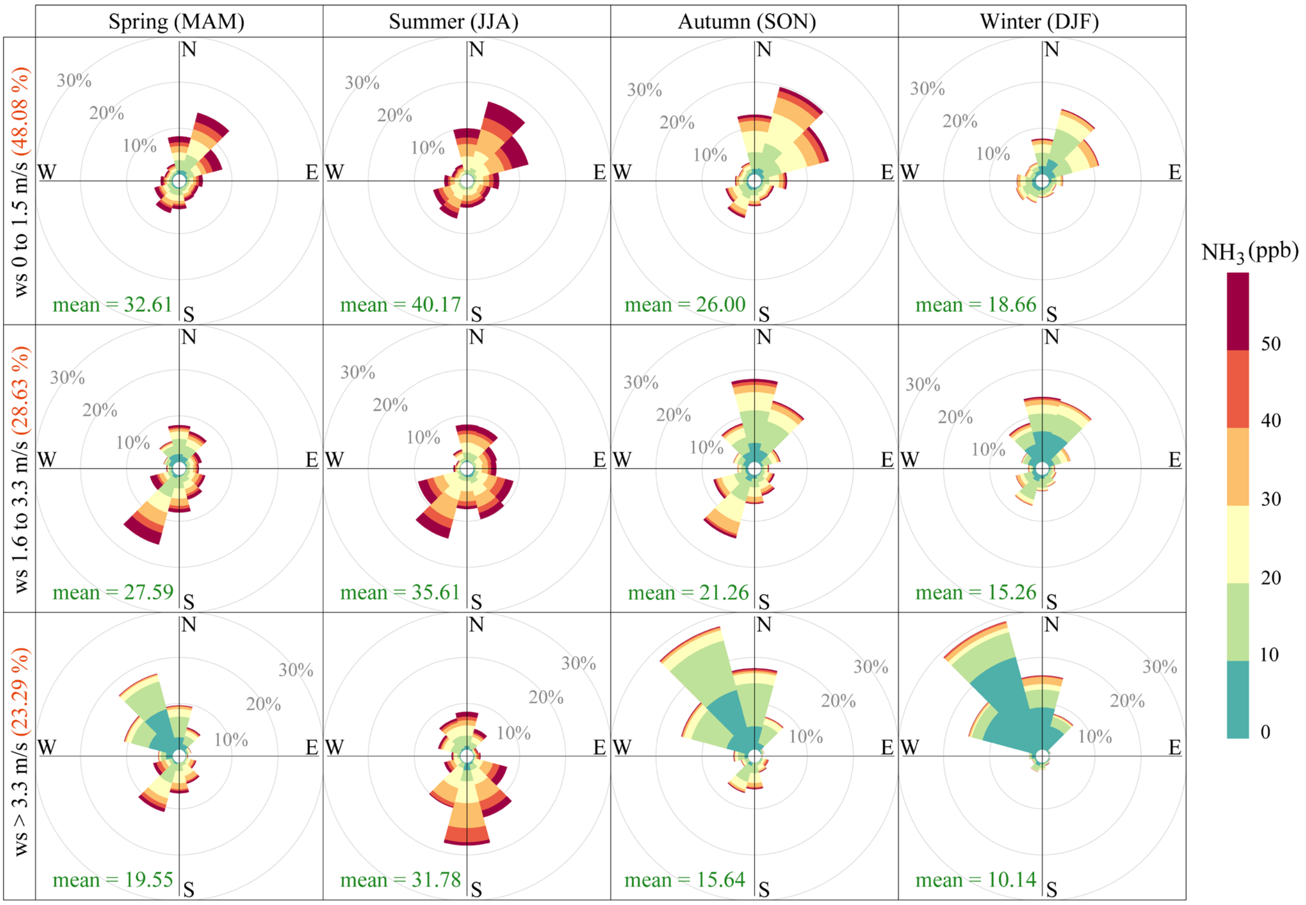

Figure S14. Pollution rose diagram of Beijing for various wind speeds in various seasons.

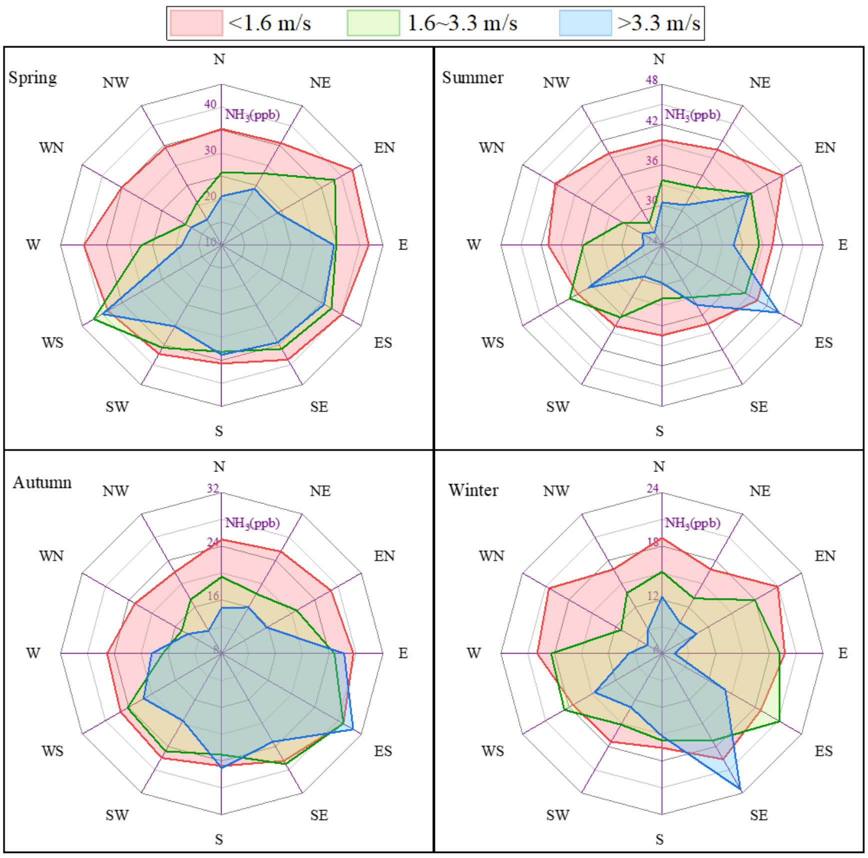

Figure S15. Mean mixing ratios of NH_3 in different wind directions under different wind speed conditions.

Table S1. Comparison of surface NH_3 mixing ratios in urban areas with monitoring results from this study (ppb).

Period	Location	Method	Result	Reference
2009/6~2020/7	Beijing, China	EC9842 NO_x/NH_3 analyzer & LGR EAA NH_3 analyzer	26.62	This study
2008/2~2008/12	Beijing, China	Ogawa passive samplers	15.3	Meng et al. (2011) [1]
2009			19.5	
2010/1~2010/7			21.0	
2013/11~2013/12	Beijing, China	17i ammonia analyzer	25.30	Zhao et al. (2016) [2]
2016/11~2016/12	Beijing, China	LGR NH_3 analyzer (DTL-100)	16.50	Wang et al. (2019) [3]
2016/4~2016/5	Beijing, China	MARGA online monitor	26.58	Su et al. (2021) [4]
2017/10~2017/11			21.04	
2017/12~2018/2			5.28	
2017/9~2018/8	Beijing, China	LGR NH_3 analyzer (907)	24.8	Pu et al. (2020) [5]
2019/3~2020/2	Beijing, China	Picarro laser spectrometer (G2103)	22.8	Gu et al. (2022) [6]
2020/5~2021/6	Beijing, China	Picarro laser spectrometer (G2103)	23.1	Sun et al. (2023) [7]
2020/9~2021/8	Beijing, China	Picarro laser spectrometer (G2103)	20.9	Gu et al. (2022) [8]
2015/9~2016/9	Beijing, China	Diffusive samplers	19.0	Pan et al. (2018) [9]
	Tianjin, China		15.7	
	Baoding, China		21.3	
	Xiamen, China		7.2	
	Guangzhou, China		8.1	
	Nanjing, China		15.0	
	Guizhou		5.4	
2006/4~2007/4	Xi'an, China	Ogawa passive samplers	17.93	Cao et al. (2009) [10]
2014/4~2015/4	Shanghai, China	MARGA online monitor	7.70	Chang et al. (2016) [11]
2014/5~2015/6	Shanghai, China	Ogawa passive samplers	7.80	Chang et al. (2019) [12]
2017/4~2018/3	Chengdu, China	Ion Chromatography (Dionex ICS-600)	13.48	Huang et al. (2021) [13]
2001/5~2002/3	Rome, Italy	Annular diffusion denuders	5.1	Perrino et al. (2002) [14]
2008/9~2009/8	Kobe, Japan	Passive sampler	2.22	Nguyen et al. (2021) [15]
2010/3~2011/3	Toronto, Canada	Passive sampler	2.74	Zbieranowski et al. (2012) [16]
2010/9~2011/8	Seoul, South Korea	Picarro laser spectrometer (G1103)	12.30	Phan et al. (2013) [17]
2012/10~2013/9	Delhi, India	Handy sampler (Envirotech model APM 821)	56.2	Singh et al. (2014) [18]
2013/1~2014/12	Delhi, India	AC32M-CNH3 analyzer	21.2	Kotnala et al. (2020) [19]
2013	Delhi, India	Serinus 44 ammonia analyzer	55.6	Saraswati et al. (2019) [20]
2014			52.4	
2015			52.2	
2016/4~2017/10	Rochester, USA	Annular diffusion denuders	2.84	Zhou et al. (2019) [21]
2016/6~2017/10	New York City, USA		3.22	
2019/5~2020/4	Jeonju, South Korea	Picarro laser spectrometer (G2103)	10.50	Park et al. (2021) [22]
2019/12~2021/9	Reims, France	Picarro laser spectrometer (G2103)	6.30	Chatain et al. (2022) [23]

Table S2. The proportion of mass concentration of each component of SNA in Beijing urban area (%)

Year	Season	SO_4^{2-}	NO_3^-	NH_4^+
2019	Spring	27.41	49.82	23.78
2009	Summer	55.14	26.47	18.39
2009	Autumn	67.03	19.17	13.80
2018	Autumn	24.91	52.07	24.02
2016	Winter	32.31	42.38	25.30
2019	Winter	25.66	48.36	26.98

Table S3. Sensitivity analysis of SNA to changes in precursor concentration.

Simulated situation	Spring				Summer			
	SO_4^{2-}	NO_3^-	NH_4^+	SNA	SO_4^{2-}	NO_3^-	NH_4^+	SNA
+0.2TS	0.20	0.04	0.36	0.21	0.20	0.03	0.49	0.12
-0.2TS	-0.20	0.25	-0.29	-0.10	-0.20	-0.02	-0.33	-0.19
+0.2TN	0.00	0.26	0.23	0.10	0.00	0.19	0.02	0.01
-0.2TN	0.00	-0.22	-0.21	-0.10	0.00	-0.19	-0.01	-0.02
+0.2TA	0.00	0.03	0.05	0.01	0.00	0.09	0.02	0.00
-0.2TA	0.00	-0.04	-0.06	-0.01	0.00	-0.10	-0.02	-0.01
Simulated situation	**Autumn**				**Winter**			
	SO_4^{2-}	NO_3^-	NH_4^+	SNA	SO_4^{2-}	NO_3^-	NH_4^+	SNA
+0.2TS	0.20	0.01	0.24	0.09	0.20	-0.00	0.15	0.08
-0.2TS	-0.20	-0.00	-0.06	-0.10	-0.20	-0.00	-0.18	-0.09
+0.2TN	0.00	0.20	0.55	0.12	0.00	0.20	0.14	0.13
-0.2TN	0.00	-0.20	-0.17	-0.12	0.00	-0.20	-0.14	-0.13
+0.2TA	0.00	0.00	0.01	0.00	-0.00	0.00	0.01	0.00
-0.2TA	0.00	-0.01	-0.02	-0.00	0.00	-0.00	-0.01	-0.00

Reference

(1) Meng, Z. Y.; Lin, W. L.; Jiang, X. M.; Yan, P.; Wang, Y.; Zhang, Y. M.; Jia, X. F.; Yu, X. L. Characteristics of Atmospheric Ammonia over Beijing, China. *Atmos Chem Phys* **2011**, *11* (12), 6139–6151. https://doi.org/10.5194/acp-11-6139-2011.

(2) Zhao, M.; Wang, S.; Tan, J.; Hua, Y.; Wu, D.; Hao, J. Variation of Urban Atmospheric Ammonia Pollution and Its Relation with $PM_{2.5}$ Chemical Property in Winter of Beijing, China. *Aerosol Air Qual Res* **2016**, *16* (6), 1390–1402. https://doi.org/10.4209/aaqr.2015.12.0699.

(3) Wang, Q.; Zhang, Q.; Ma, Z.; Ge, B.; Xie, C.; Zhou, W.; Zhao, J.; Xu, W.; Du, W.; Fu, P.; Lee, J.; Nemitz, E.; Cowan, N.; Mullinger, N.; Cheng, X.; Zhou, L.; Yue, S.; Wang, Z.; Sun, Y. Temporal Characteristics and Vertical Distribution of Atmospheric Ammonia and Ammonium in Winter in Beijing. *Science of The Total Environment* **2019**, *681*, 226–234. https://doi.org/10.1016/j.scitotenv.2019.05.137.

(4) Su, J.; Zhao, P.; Ding, J.; Du, X.; Dou, Y. Insights into Measurements of Water-Soluble Ions in $PM_{2.5}$ and Their Gaseous Precursors in Beijing. *Journal of Environmental Sciences* **2021**, *102*, 123–137. https://doi.org/10.1016/j.jes.2020.08.031.

(5) Pu, W.; Ma, Z.; Collett Jr, J. L.; Guo, H.; Lin, W.; Cheng, Y.; Quan, W.; Li, Y.; Dong, F.; He, D. Regional Transport and Urban Emissions Are Important Ammonia Contributors in Beijing, China. *Environ Pollut* **2020**, *265*, 115062. https://doi.org/10.1016/j.envpol.2020.115062.

(6) Gu, M.; Pan, Y.; Walters, W. W.; Sun, Q.; Song, L.; Wang, Y.; Xue, Y.; Fang, Y. Vehicular Emissions Enhanced Ammonia Concentrations in Winter Mornings: Insights from Diurnal Nitrogen Isotopic Signatures. *Environ Sci Technol* **2022**, *56* (3),

1578–1585. https://doi.org/10.1021/acs.est.1c05884.

(7) Sun, Q.; Gu, M.; Wu, D.; Yang, T.; Wang, H.; Pan, Y. Concurrent Measurements of Atmospheric Ammonia Concentrations in the Megacities of Beijing and Shanghai by Using Cavity Ring-down Spectroscopy. *Atmos Environ* **2023**, *307*, 119848. https://doi.org/10.1016/j.atmosenv.2023.119848.

(8) Gu, M.; Pan, Y.; Sun, Q.; Walters, W. W.; Song, L.; Fang, Y. Is Fertilization the Dominant Source of Ammonia in the Urban Atmosphere? *Science of The Total Environment* **2022**, *838*, 155890. https://doi.org/10.1016/j.scitotenv.2022.155890.

(9) Pan, Y.; Tian, S.; Zhao, Y.; Zhang, L.; Zhu, X.; Gao, J.; Huang, W.; Zhou, Y.; Song, Y.; Zhang, Q.; Wang, Y. Identifying Ammonia Hotspots in China Using a National Observation Network. *Environ Sci Technol* **2018**, *52* (7), 3926–3934. https://doi.org/10.1021/acs.est.7b05235.

(10) Cao, J.-J.; Zhang, T.; Chow, J. C.; Watson, J. G.; Wu, F.; Li, H. Characterization of Atmospheric Ammonia over Xi'an, China. *Aerosol Air Qual Res* **2009**, *9* (2), 277–289. https://doi.org/10.4209/aaqr.2008.10.0043.

(11) Chang, Y.; Zou, Z.; Deng, C.; Huang, K.; Collett, J. L.; Lin, J.; Zhuang, G. The Importance of Vehicle Emissions as a Source of Atmospheric Ammonia in the Megacity of Shanghai. *Atmos Chem Phys* **2016**, *16* (5), 3577–3594. https://doi.org/10.5194/acp-16-3577-2016.

(12) Chang, Y.; Zou, Z.; Zhang, Y.; Deng, C.; Hu, J.; Shi, Z.; Dore, A. J.; Collett, J. L. Assessing Contributions of Agricultural and Nonagricultural Emissions to Atmospheric Ammonia in a Chinese Megacity. *Environ Sci Technol* **2019**, *53* (4), 1822–1833. https://doi.org/10.1021/acs.est.8b05984.

(13) Huang, X.; Zhang, J.; Zhang, W.; Tang, G.; Wang, Y. Atmospheric Ammonia and Its Effect on $PM_{2.5}$ Pollution in Urban Chengdu, Sichuan Basin, China. *Environ Pollut* **2021**, *291*, 118195. https://doi.org/10.1016/j.envpol.2021.118195.

(14) Perrino, C.; Catrambone, M.; Di Menno Di Bucchianico, A.; Allegrini, I. Gaseous Ammonia in the Urban Area of Rome, Italy and Its Relationship with Traffic Emissions. *Atmos Environ* **2002**, *36* (34), 5385–5394. https://doi.org/10.1016/s1352-2310(02)00469-7.

(15) Nguyen, D. V.; Sato, H.; Hamada, H.; Yamaguchi, S.; Hiraki, T.; Nakatsubo, R.; Murano, K.; Aikawa, M. Symbolic Seasonal Variation Newly Found in Atmospheric Ammonia Concentration in Urban Area of Japan. *Atmos Environ* **2021**, *244*, 117943. https://doi.org/10.1016/j.atmosenv.2020.117943.

(16) Zbieranowski, A. L.; Aherne, J. Ambient Concentrations of Atmospheric Ammonia, Nitrogen Dioxide and Nitric Acid across a Rural–Urban–Agricultural Transect in Southern Ontario, Canada. *Atmos Environ* **2012**, *62*, 481–491. https://doi.org/10.1016/j.atmosenv.2012.08.040.

(17) Phan, N.-T.; Kim, K.-H.; Shon, Z.-H.; Jeon, E.-C.; Jung, K.; Kim, N.-J. Analysis of Ammonia Variation in the Urban Atmosphere. *Atmos Environ* **2013**, *65*, 177–185. https://doi.org/10.1016/j.atmosenv.2012.10.049.

(18) Singh, S.; Kulshrestha, U. C. Rural versus Urban Gaseous Inorganic Reactive Nitrogen in the Indo-Gangetic Plains (IGP) of India. *Environ Res Lett* **2014**, *9* (12), 125004. https://doi.org/10.1088/1748-9326/9/12/125004.

(19) Kotnala, G.; Sharma, S. K.; Mandal, T. K. Influence of Vehicular Emissions (NO, NO_2, CO and NMHCs) on the Mixing Ratio of Atmospheric Ammonia (NH_3) in Delhi, India. *Arch Environ Con Tox* **2019**, *78* (1), 79–85. https://doi.org/10.1007/s00244-019-00689-8.

(20) Saraswati; George, M. P.; Sharma, S. K.; Mandal, T. K.; Kotnala, R. K. Simultaneous Measurements of Ambient NH_3 and Its Relationship with Other Trace Gases, $PM_{2.5}$ and Meteorological Parameters over Delhi, India. *MAPAN* **2019**, *34* (1), 55–69. https://doi.org/10.1007/s12647-018-0286-0.

(21) Zhou, C.; Zhou, H.; Holsen, T. M.; Hopke, P. K.; Edgerton, E. S.; Schwab, J. J. Ambient Ammonia Concentrations Across New York State. *J Geophys Res-atmos* **2019**, *124* (14), 8287–8302. https://doi.org/10.1029/2019jd030380.

(22) Park, J.; Kim, E.; Oh, S.; Kim, H.; Kim, S.; Kim, Y. P.; Song, M. Contributions of Ammonia to High Concentrations of

PM2.5 in an Urban Area. *Atmosphere-basel* **2021**, *12* (12), 1676. https://doi.org/10.3390/atmos12121676.

(23) Chatain, M.; Chretien, E.; Crunaire, S.; Jantzem, E. Road Traffic and Its Influence on Urban Ammonia Concentrations (France). *Atmosphere-basel* **2022**, *13* (7), 1032. https://doi.org/10.3390/atmos13071032.

(24) Huang, X., Song, Y., Li, M., Li, J., Huo, Q., Cai, X., Zhu, T., Hu, M., and Zhang, H.: A high-resolution ammonia emission inventory in China, Global Biogeochem Cy **2012**, 26, GB1030. https://doi.org/10.1029/2011gb004161.

(25) Kang, Y., Liu, M., Song, Y., Huang, X., Yao, H., Cai, X., Zhang, H., Kang, L., Liu, X., Yan, X., He, H., Zhang, Q., Shao, M., and Zhu, T.: High-resolution ammonia emissions inventories in China from 1980 to 2012, Atmos Chem Phys **2016**, 16, 2043–2058. https://doi.org/10.5194/acp-16-2043-201.

(26) Hersbach, H., Bell, B., Berrisford, P., Biavati, G., Horányi, A., Muñoz Sabater, J., Nicolas, J., Peubey, C., Radu, R., Rozum, I., Schepers, D., Simmons, A., Soci, C., Dee, D., Thépaut, J-N.: ERA5 hourly data on single levels from 1940 to present. Copernicus Climate Change Service (C3S) Climate Data Store (CDS) **2023**. https://doi.org/10.24381/cds.adbb2d47.